

A three-state hyperthermic cell death model for the prediction of myocardial lesion[★]

Stefan Lämmermann^{*} Argyrios Petras^{**}
 Massimiliano Leoni^{**} Jose M. Guerra^{***}
 Luca Gerardo-Giorda^{**,*}

^{*} Johannes Kepler University, Linz, 4020 Austria

^{**} RICAM - Johann Radon Institute for Computational and Applied Mathematics, Linz, 4020 Austria (e-mail: argyrios.petras@ricam.oeaw.ac.at).

^{***} Hospital de la Santa Creu i San Pau, IIB Sant Pau, Universitat Autònoma de Barcelona, Barcelona, 08025 Spain

1. INTRODUCTION

Radiofrequency (RF) catheter ablation is a minimally invasive procedure commonly used for the treatment of cardiac arrhythmias. Though it has been effectively practiced for many years, this procedure is not exempt from complications, including charring formation due to blood overheating at temperatures higher than 80°C and the occurrence of steam pops for tissue temperatures around 100°C. Several models have been introduced to simulate the RF ablation procedure, which provide lesion size estimations at the end of the ablation. Typically, either the 50°C isotherm is considered as an estimation for the lesion, or an Arrhenius type model, which accounts for the time at which the tissue is at an altered state. In this work a three-state cell death model is considered for the estimation of the lesion, which captures the shrinkage of the damage region after the completion of the ablation.

2. METHODS

2.1 Three-state cell death model

The model introduced in Park et al. (2016) considers three states for the proteins within the cell: Native (N), Unfolded (U) and Denaturated (D). The dynamics are described as follows:

$$\begin{aligned}
 & N \xrightleftharpoons[k_3]{k_1} U \xrightarrow{k_2} D, \\
 & \frac{dN}{dt} = -k_1 N + k_3 U, \\
 & \frac{dU}{dt} = k_1 N - k_3 U - k_2 U, \\
 & \frac{dD}{dt} = k_2 U,
 \end{aligned} \tag{1}$$

where k_1 , k_2 and k_3 follow the Arrhenius model

^{*} AP, ML and LGG were partially supported by the State of Upper Austria.

$$k_i = A_i e^{-\Delta E_i / (RT)}, \quad i = 1, 2, 3,$$

with A_i being the frequency factor, ΔE_i the activation energy, R the universal gas constant and T the temperature. Note that at all times $N + U + D = 1$. The system (1) is solved numerically using the Runge-Kutta third-order method and $\Delta t = 0.01$. This scheme allows for the conservation the quantity $N + U + D$ at all times.

2.2 Slow cell death dynamics

While for fast cell death dynamics equation (1) is capable of capturing the denaturation behavior for the rapid changes that occur during thermal ablation treatments, experimental data show that the cell viability decreases at a much slower pace in comparison to the duration of the procedure. In particular, experimental evidence on human liver hepatocellular carcinoma cells and human lung fibroblasts show that once cells receive thermal damage beyond some given threshold (i.e. the native proteins are below a threshold N_{thr}), they progressively reach a denaturated state. Following ONeill et al. (2011), we consider a threshold value of $N_{thr} = 80\%$.

3. RESULTS

3.1 Calibration

While experimental results exist for different types of cells, including bovine chordae tendineae (Park et al. (2016)), human liver hepatocellular carcinoma and human lung fibroblasts (ONeill et al. (2011)), no data are available for the estimation of the 6 parameters for the hyperthermic death of cardiac myocytes. To tune the parameters for such cells, we consider that thermal damage occurs at temperatures higher than 43°C, however the tissue damage is reversible for heating up to 48°C and exposure time of 60s (Zaltieri et al. (2021)). Additionally, the mean frequency A and activation energy ΔE defined as

$$\Delta E = \Delta E_1 + \Delta E_2 - \Delta E_3 \quad \text{and} \quad A = \frac{A_1 A_2}{A_3},$$

should lie within the physiological ranges of $100 - 800 \text{ kJ/mol}$ and $10^9 - 10^{129} \text{ s}^{-1}$ found in the literature and the values given in Park et al. (2016) for proteins.

3.2 Application to RF ablation

Next, we apply the computational model to the simulated results obtained in Petras et al. (2019) using a 3D computational framework. The simulation protocol employs 30s of ablation followed by 30s of relaxation, where no ablation is performed and the saline irrigation rate drops to standby mode of 2 mL/min . We consider the three ablation protocols that have been used for validation, namely $(10g, 20W)$, $(10g, 35W)$ and $(20g, 20W)$, indicating the contact force in g and the applied power in W . The results after the completion of 60s appear in Figure 1 for the parameter set in Table 1 (A_i in s^{-1} and ΔE_i in kJ/mol , $i = 1, 2, 3$).

Table 1. The parameter set chosen for the three-state model.

A_1	ΔE_1	A_2	ΔE_2	A_3	ΔE_3
3.68×10^{30}	200.1	5.68×10^3	40.6	2.85×10^9	43

We get a good agreement with the experimental data shown in Petras et al. (2019) for the depth (D) and the depth at the maximum width (DW), while the simulated lesion underestimates the width (W), which is consistent with the observations in Petras et al. (2019) for the ablation protocols $(10g, 20W)$ and $(20g, 20W)$ using the 50°C isotherm. On the other hand, the D and DW are slightly outside the experimental ranges in the case of $(10g, 35W)$. This is consistent with the 50°C isotherm lesion estimation, since the measurements were close to the limits of the range of the observed experimental data. This might possibly happen due to the underestimation of the thermal conductivity of the tissue for large temperature values (maximum tissue temperature $T = 87^\circ\text{C}$), due to the lack of data available in the literature (available data appear only for temperatures lower than 76°C).

4. CONCLUSION

The calibrated three-state hyperthermic cell death model is capable of capturing the shrinkage of the damaged tissue area after the ablation, simulating the reversible damage that occurs, while accounting for the slow cell death. Additionally, our results indicate that the 50°C isotherm is overestimating the lesion size.

5. LIMITATIONS

Limitations of this study include the lack of experimental data for the validation of the thermal cell death for cardiac myocytes. While other parameters might satisfy the model calibration, we considered a parameter set that is producing lesions that are within the experimental measurements provided by Petras et al. (2019).

REFERENCES

ONEILL, D.P., Peng, T., Stiegler, P., Mayrhauser, U., Koestenbauer, S., Tscheliessnigg, K., and Payne, S.J.

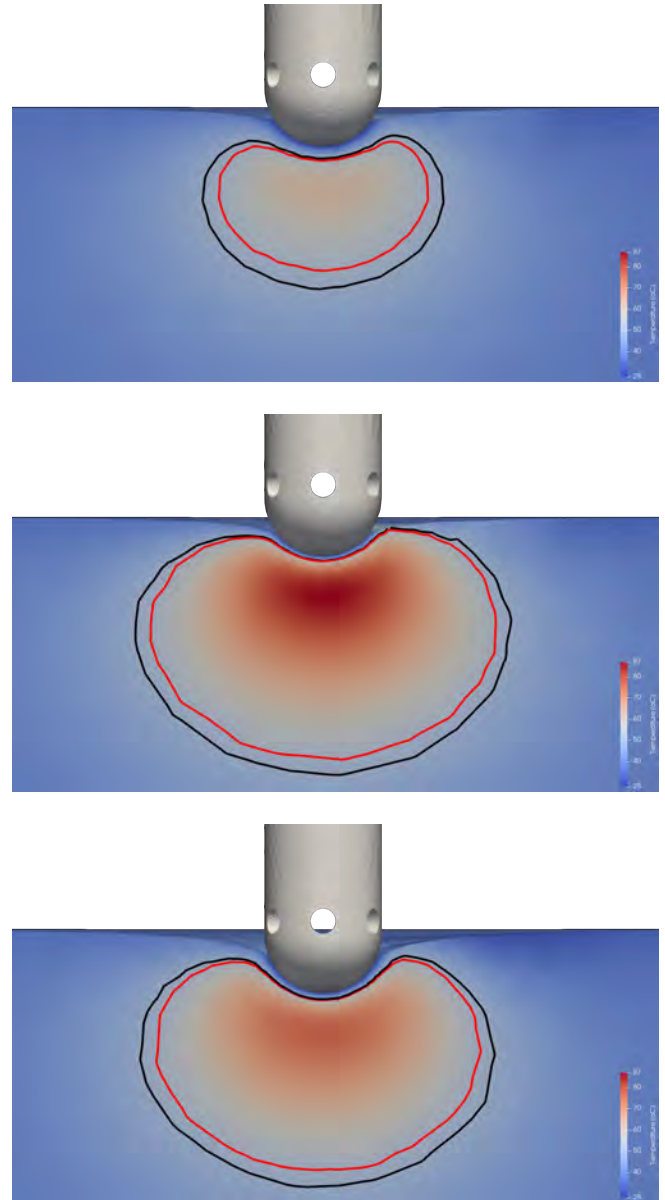


Fig. 1. The lesion size estimation using the 50°C isotherm (black line) versus the $N_{thr} = 80\%$ contour from the three-state model (red line) for the cases of $(10g, 20W)$ (top), $(10g, 35W)$ (middle) and $(20g, 20W)$ (bottom).

(2011). A three-state mathematical model of hyperthermic cell death. *Annals of biomedical engineering*, 39(1), 570–579.

Park, C.S., Hall, S.K., Liu, C., and Payne, S.J. (2016). A model of tissue contraction during thermal ablation. *Physiological measurement*, 37(9), 1474.

Petras, A., Leoni, M., Guerra, J.M., Jansson, J., and Gerardo-Giorda, L. (2019). A computational model of open-irrigated radiofrequency catheter ablation accounting for mechanical properties of the cardiac tissue. *International Journal for Numerical Methods in Biomedical Engineering*, 35(11), e3232.

Zaltieri, M., Massaroni, C., Cauti, F.M., and Schena, E. (2021). Techniques for temperature monitoring of myocardial tissue undergoing radiofrequency ablation treatments: An overview. *Sensors*, 21(4), 1453.